JASA EXPRESS LETTERS

Ultra-sparse near-perfect sound absorbers

Cite as: JASA Express Lett. **3**, 034001 (2023); https://doi.org/10.1121/10.0017520
Submitted: 23 December 2022 • Accepted: 18 February 2023 • Published Online: 13 March 2023

Jun Ji, Junfei Li, Steven A. Cummer, et al.

JASA EXPRESS LETTERS ARTICLE asa.scitation.org/journal/jel

Ultra-sparse near-perfect sound absorbers

Jun Ji,[1] Junfei Li,[2] Steven A. Cummer,[2] and Yun Jing[1,a)]
[1]Graduate Program in Acoustics, The Pennsylvania State University, University Park, Pennsylvania 16802, USA
[2]Department of Electrical and Computer Engineering, Duke University, Durham, North Carolina 27708, USA
jbj5431@psu.edu, junfei.li@duke.edu, cummer@ee.duke.edu, yqj5201@psu.edu

Abstract: There is a trade-off between the sparseness of an absorber array and its sound absorption imposed by wave physics. Here, near-perfect absorption (99% absorption) is demonstrated when the spatial period of monopole-dipole resonators is close to one working wavelength (95% of the wavelength). The condition for perfect absorption is to render degenerate monopole-dipole resonators critically coupled. Frequency domain simulations, eigenfrequency simulations, and the coupled mode theory are utilized to demonstrate the acoustic performances and the underlying physics. The sparse-resonator-based sound absorber could greatly benefit noise control with air flow and this study could also have implications for electromagnetic wave absorbers.

[Editor: Siu-Kit Lau] https://doi.org/10.1121/10.0017520

Received: 23 December 2022 Accepted: 18 February 2023 Published Online: 13 March 2023

1. Introduction

Noise control methods that rely on sound absorption/reflection while preserving ventilation is of great interest[1] for many occasions: automobile mufflers,[2] room windows,[3] sound barriers[4–7] and cages,[8–10] etc. In pursuit of ventilated sound absorbers, in particular, the conventional solution is to design an acoustic dissipative liner using fibrous materials,[11] perforated panels with backing cavities,[12,13] or both.[14] However, these acoustic liners are often bulky and cannot achieve strong absorption, such as near-perfect absorption.

Perfect absorption with a subwavelength structure[15] has been made possible recently by acoustic metamaterials[16] and acoustic metasurfaces[17] based on the enhanced local resonance and impedance matching. In fact, there is an intrinsic trade-off between the efficiency of sound absorption and ventilation,[18] which means that a strong ventilation generally implies a poor absorption. For ducts or absorber arrays whose width or periodicity is limited to half wavelength, only the fundamental propagating mode exists and perfect absorption in such a scenario[19–24] can be realized, either by harnessing a hybrid resonance composed of both monopole (symmetric) and dipole (anti-symmetric) resonances,[19,20] or by a pair of coupled resonances creating a "soft" wall.[21,24,25] More recently, there is a trend to pursue a maximum periodicity under the condition of perfect absorption to advance the efficiency of ventilation. Lee et al.[26] derived an upper limit on the periodicity of a perfect absorber array, that is $\delta 2=p\text{Þ}k_0$, and demonstrated it with an absorber unit composed a pair of lossy and lossless resonators. Along this direction, Su et al.[27] extended the periodicity limit to $0{:}88k_0$ by using a degenerate monopole and dipole resonances. Lapin[28] attempted the theoretical derivations of the periodicity for a perfect absorber array around two decades ago and showed that for a periodicity smaller than k_0, the condition for perfect absorption of a plane wave incidence is to render degenerate monopole-dipole resonators critically coupled. However, no real-structure design has been presented to support this periodicity limit of k_0.

In this study, we analytically and numerically show an ultra-sparse absorber array with a periodicity of $d ¼ 0{:}95k_0$ achieving near-perfect (99%) absorption. Such an ultra-sparse near-perfect sound absorber array is realized with pairs of monopole-dipole resonators. Instead of using a highly coupled resonance by Su et al.,[27] the capability to separately control the pair of monopole and dipole resonators helps the simultaneous realization of degeneracy and critical coupling for perfect absorption as the absorber array approaches the theoretical limit for the periodicity. With parameters of eigenfrequency, leakage loss, and dissipation loss being retrieved from the Eigenfrequency study of COMSOL, the analytical calculation of absorption coefficient shows a good agreement with the numerical result.

2. Schematic and design

Figure 1(a) shows a 3D schematic of an ultra-sparse near-perfect absorber array for the frequency of interest f_0, which is considered to be 3000 Hz in this study. A plane wave normal to the array is incident along the x direction. The periodicity of the array along y direction is $d ¼ 0{:}95k_0$. The array is uniform along the z direction. Each unit cell of the array is

a)Author to whom correspondence should be addressed.

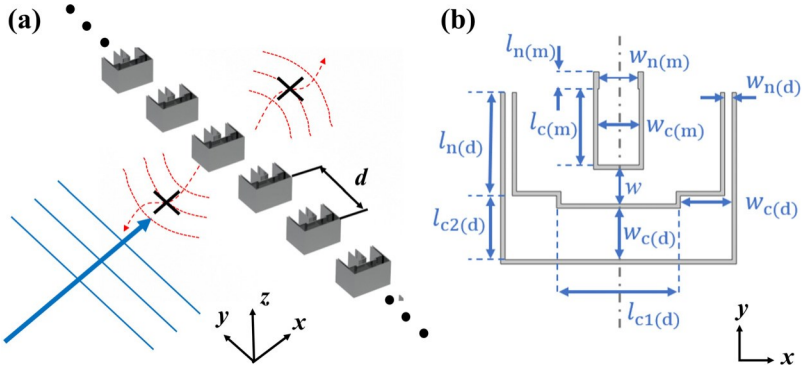

Fig. 1. (a) 3 D schematic of an ultra-sparse near-perfect absorber array. (b) Cross-sectional geometry of each unit cell of the array, which is composed of a Helmholtz resonator as a monopole resonator and a space-coiled open-open tube as a dipole resonator. The vertical dash-dotted line in gray is the plane of mirror symmetry.

composed of a monopole resonator and a dipole resonator, which can be characterized by their eigenfrequency $f_{m=d}$, leak-age loss rate $c_{m=d}$, and dissipation loss rate $d_{m=d}$ in Sec. 3. The coupling between two resonators is minimal and negligible since the monopole and dipole resonators have opposite symmetry properties. Figure 1(b) shows the geometry for the unit cell in the x-y plane. The monopole resonator is realized by a Helmholtz resonator, with neck length $l_{n\delta m\flat}$, neck width $w_{n\delta m\flat}$, cavity length $l_{c\delta m\flat}$, and cavity width $w_{c\delta m\flat}$. The dipole resonator is realized by a space-coiled open-open tube, with neck length $l_{n\delta d\flat}$, neck width $w_{n\delta d\flat}$, cavity length $l_{c1\delta d\flat}$, and $l_{c2\delta d\flat}$, and cavity width $w_{c\delta d\flat}$. The monopole and dipole resona-tors are separated by a decent distance w to avoid a strong thermoviscous loss in the channel region between the two reso-nators so that the thermoviscous loss exists in a controlled manner inside the resonators. The mathematical interpretation for the conditions of degeneracy and critical coupling is

$$f_m \text{ ¼ } f_d; \quad d_m \text{ ¼ } c_m; \quad d_d \text{ ¼ } c_d: \tag{1}$$

The geometric parameters of our absorber array listed in Table 1 comes from a two-step design strategy. With the required conditions in Eq. (1), an initial design is first brought up from an educated guess in which the monopole and dipole unit cell have a resonance frequency f_0. Then, the Optimization module in COMSOL MULTIPHYSICS version 6.0 is used with a target to maximize the absorption A at f_0. Geometric parameters including neck length, neck width, cavity length, and cavity width for the monopole and dipole resonators are set as design variables. The constraints include $A_{m=d} >$ const. That is, the absorption for the monopole and the dipole is larger than a constant value. The efficiency of the optimization depends on the constant value, and we set it as 0.4. More details about COMSOL setup are discussed in the last paragraph of this section. Different initial designs (e.g., resonators with difference neck widths and cavity widths but having the same resonant frequency f_0) from the educated guess are optimized until the total absorption reaches 99%.

For ventilated absorbers without a rigid backing, at most 50%[29,30] of the incident power can be absorbed if the absorber supports a single resonance for a single-sided incident wave. Figure 2(a) shows the numerical absorption coeffi-cient as a function of geometry modulation Dl_n and Dw_n for our designed monopole (left) and dipole (right) resonator when the other resonator is closed. In other words, when studying the monopole behavior, the dipole is physically dis-abled, and vice versa. When Dl_n ¼ 0 and Dw_n ¼ 0, the monopole and dipole resonators separately absorb around 50% absorption at 3000 Hz. In order to have a perfect absorption in such scenario, the absorber is designed to support both two resonances which are degenerate in frequency but have opposite symmetry with respect to the mirror plane of the sys-tem. As shown in Fig. 2(b), absorption coefficient reaches 99% at 3000 Hz when both the monopole and dipole resonators are interacting with the incident wave. The absorption peak near 3150 Hz is resulted from an undesired mode when the periodicity is equal to one wavelength, which causes the absorption for the single resonance at 3000 Hz being a little bit larger than the maximum limit 50%. Similar to waveguide modes caused by periodically repeated rigid walls, this unde-sired mode is a general mode caused by the general periodic boundary condition. This undesired mode is also a roadblock to approaching the periodicity limit, since more than two modes are around the frequency of interest. Thus, to render degenerate monopole-dipole resonators critically coupled in a more extreme case, such as d ¼ 0:99k_0, is hard, and optimi-zation on more than two degenerate modes is needed. Figure 2(c) shows the distributions of acoustic pressure in color

Table 1. The geometric parameters of our design in Fig. 1(b). The unit is in mm.

$l_{n(m)}$	$w_{n(m)}$	$l_{c(m)}$	$w_{c(m)}$	$l_{n(d)}$	$w_{n(d)}$	$l_{c1(d)}$	$l_{c2(d)}$	$w_{c(d)}$	w
4	9	17.8	9.6	24	1.7	28.7	14.9	12	8

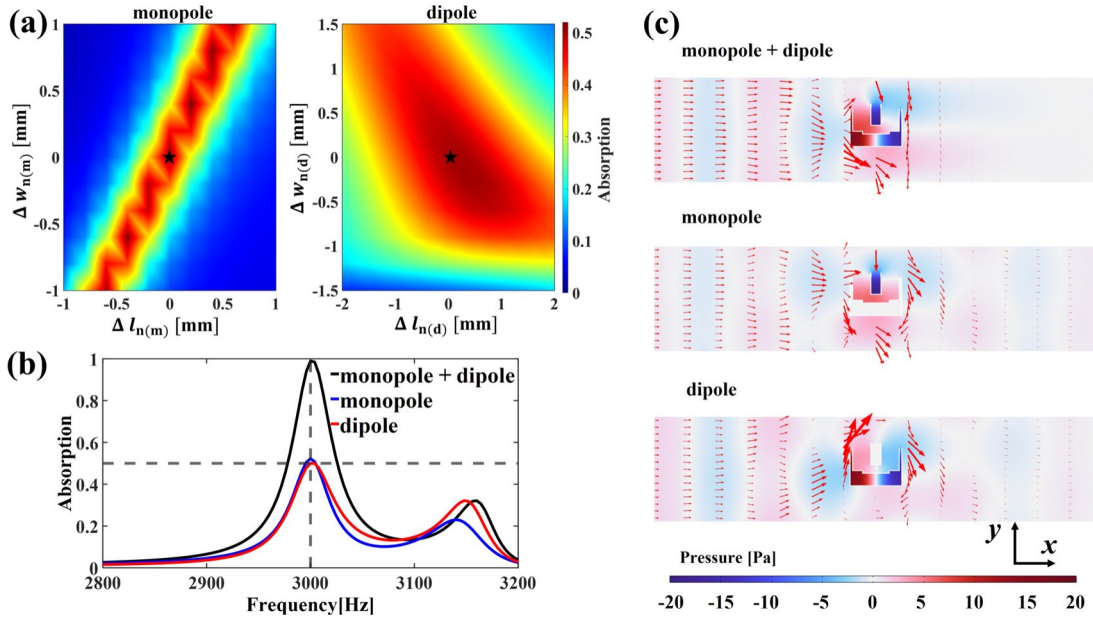

Fig. 2. (a) Numerical absorption coefficient as a function of geometry modulation Dl_n and Dw_n for monopole (left) and dipole (right) resona-tors when the other resonator is closed. (b) Numerical absorption coefficient of the optimal design [marked as black stars in (a)] in frequency domain when both monopole and dipole (black curve), only monopole (blue curve), and only dipole (red curve) resonator is functional. (c) Numerically computed distributions of acoustic pressure (color) and acoustic intensity (arrow) at 3000 Hz in a unit cell with Floquet periodic boundary condition along the y direction, when both monopole and dipole (top), only monopole (middle), and only dipole (bottom) resona-tor is functional. Magnitude of acoustic intensity is proportional to the size of arrow.

and acoustic intensity using arrows at 3000 Hz. When both resonators are functional, both acoustic pressure and acoustic intensity are extremely weak on the transmission side (or right port). If only one of them is interacting with the incident wave, acoustic pressure and acoustic intensity can be visible on the right port, indicating the transmission of energy. The y component of acoustic intensity is strong near unit cells, which indicates the repetition of unit cells along the y direction and the scattering effect between them. The dipole resonator essentially is a one wavelength resonator, and acoustic pres-sure inside has the opposite symmetry to the monopole resonator with respect to the mirror plane of the system. Because of the space-coiling, the physical length of the dipole resonator along the x direction is around half wavelength and can be further shrunk for miniaturization purposes.

The numerical study in Figs. 2(a)–2(c) is conducted in COMSOL with the Acoustic-Thermoviscous Acoustic Interaction, Frequency Domain module. The effect of the viscous friction and the heat transfer is concluded in the linearized compressible Navier–Stokes equation, the continuity equation, and the energy. Hard boundaries are imposed on the interfa-ces between air and 1 mm thick solid walls due to the large impedance mismatch between air and solid materials. No-slip and isothermal condition are applied at hard boundaries with boundary layer mesh. A normally incident plane wave with unit amplitude impinges along the þx direction, and Floquet periodic boundary condition is applied along y direction to account for the scattering between unit cells and the fact that this is an array of resonators. The absorption coefficient can be calculated by either the surface integral of the default variable ta.diss_tot in COMSOL (i.e., total thermos-viscous power dis-sipation density in W/m^3) or the line integral of the normal acoustic intensity of the reflected wave and transmitted wave.

3. Results and discussions

Eigenfrequency and the loss ratio (i.e., c=d) are retrieved using two sets of 2D Eigenfrequency studies in COMSOL.[31] One set of the Eigenfrequency study considers the thermoviscous loss, in which the real part of the eigenfrequency $f_{m=d}$ is the eigenfrequency and the imaginary part is $ðc_{m=d}Þ d_{m=d}Þ=ð2pÞ$. The other set of the Eigenfrequency study does not consider the thermoviscous loss, in which the real part of eigenfrequency $f^0_{m=d}$ is larger than the eigenfrequency $f_{m=d}$ and thus the imaginary part $c^c_{m=d}=ð2pÞ$ used for the leakage loss $c_{m=d}$ needs a revision by

$$c_{m=d} ¼ \frac{c^c_{m=d}}{f^c_{m=d}} f_{m=d}: \quad (2)$$

For both sets of the Eigenfrequency study, a Floquet periodic condition is applied along the y direction and plane wave radiation is applied at the two ports. Figures 3(a) and 3(b) show the numerical eigenfrequency and loss ratio as a function

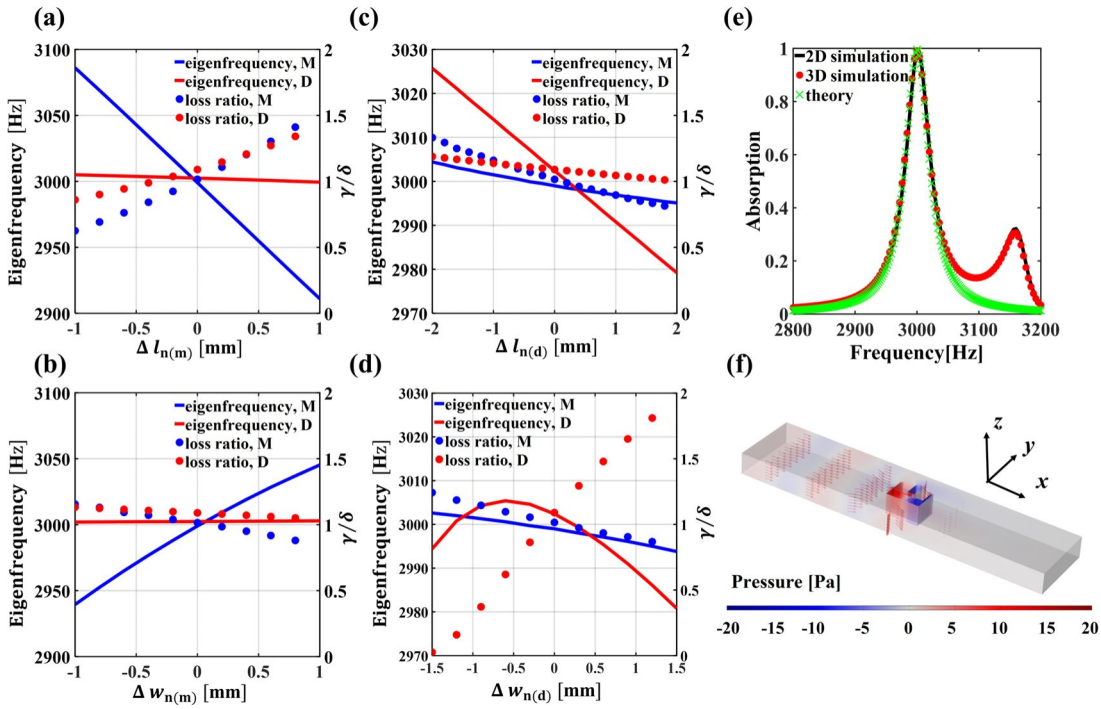

Fig. 3. Numerical eigenfrequency and loss ratio as a function of geometry modulation (a) $Dl_{n\delta m\flat}$, (b) $Dw_{n\delta m\flat}$, (c) $Dl_{n\delta d\flat}$, and (d) $Dw_{n\delta d\flat}$. (e) Absorption coefficient of the optimal design in 2D numerical simulation, 3D numerical simulation and the couple mode theory. (f) 3D numerically computed distributions of acoustic pressure (color) and acoustic intensity (arrow) at 3000 Hz, when our designed absorber is extended 3.5 cm along z direction and put inside a 3D unit cell with Floquet periodic boundary condition along y direction. Magnitude of acoustic intensity is proportional to the size of arrow.

of monopole geometry modulation $Dl_{n\delta m\flat}$ and $Dw_{n\delta m\flat}$. $Dl_{n\delta m\flat}$ and $Dw_{n\delta m\flat}$ dominantly affect the eigenfrequency and loss ratio of the monopole mode. Figures 3(c) and 3(d) show that $Dl_{n\delta d\flat}$ dominantly affects the eigenfrequency of the dipole mode, while $Dw_{n\delta d\flat}$ dominantly affects the loss factor of the dipole mode. The capability to separately control the mono-pole and dipole resonators greatly facilitates the simultaneous realization of degeneracy and critical coupling for perfect absorption as the periodicity approaches the limit. Without varying any geometry, the designed monopole-dipole absorber is degenerate and critically coupled. Plugging the retrieved parameters into the equation derived from the coupled mode theory,[29] the absorption coefficient is

$$A = \frac{2d_m c_m}{\delta x\ddot{y}\ x_m\flat^2 \flat\ \delta d_m \flat\ c_m\flat^2} \flat \frac{2d_d c_d}{\delta x\ddot{y}\ x_d\flat^2 \flat\ \delta d_d \flat\ c_d\flat^2}: \tag{3}$$

The theoretical prediction has a great agreement with both 2D and 3D simulations near 3000 Hz, as shown in Fig. 3(e). The 3D simulation is conducted with our designed absorber being extended 3.5 cm along the z direction and Fig. 3(f) shows a 3D distribution of acoustic pressure (color) and acoustic intensity (arrow) at 3000 Hz. The discrepancy between the theoretical model and numerical models is because the modes near 3150 Hz are not considered in the theory.

It should be pointed out that such an ultra-sparse near perfect absorber is designed at the cost of being sensitive to the angle of incidence as shown in Fig. 4. The absorption coefficient drops significantly as the oblique incident angle increases to 4. To mitigate this issue, one could use rigid walls as a special kind of periodic condition instead of the Floquet periodic boundary condition, which is what we are using now in the numerical model. This would render the problem an absorption problem in a waveguide with only a few propagation modes, i.e., discrete incident wave components. In addition, porous materials with high dissipation loss could be used to broaden the absorption bandwidth to make the design less sensitive to the incident angle.

4. Conclusion

In this study, we analytically and numerically show that an ultra-sparse absorber array with a periodicity of $d = 0.95k_0$ can achieve near-perfect (99%) absorption at the designed frequency f_0. Such an ultra-sparse near-perfect sound absorber array is realized with an array of monopole-dipole paired resonators. By separately controlling the monopole and dipole resonators, simultaneous realization of degeneracy and critical coupling which are crucial for perfect absorption can be realized as the absorber array approaches the limit for the periodicity. With parameters of eigenfrequency, leakage loss,

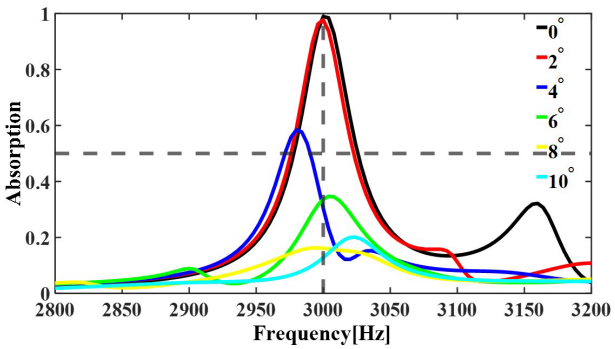

Fig. 4. Absorption coefficient as a function of frequency and the angle of incidence in 2D numerical simulations.

and dissipation loss being retrieved from Eigenfrequency study of COMSOL, the analytical calculation of absorption coefficient yields a good agreement with numerical results in both 2D and 3D. The sparse-resonator-based sound absorber could greatly benefit noise control with ventilation and the results of this study could have implications for electromagnetic wave absorbers because of similarities in wave physics[29] governed by the coupled mode theory.

Acknowledgments

This work was supported by NSF CMMI Award Nos. 1951221 and 1951106.

References and links

[1]R. Dong, M. Sun, F. Mo, D. Mao, X. Wang, and Y. Li, "Recent advances in acoustic ventilation barriers," J. Phys. D 54(40), 403002 (2021).
[2]C. Wang, L. Cheng, and L. Huang, "Realization of a broadband low-frequency plate silencer using sandwich plates," J. Sound Vib. 318(4–5), 792–808 (2008).
[3]Y. Ge, H. X. Sun, S. Q. Yuan, and Y. Lai, "Switchable omnidirectional acoustic insulation through open window structures with ultrathin metasurfaces," Phys. Rev. Mater. 3(6), 065203 (2019).
[4]Y. Cheng, C. Zhou, B. G. Yuan, D. J. Wu, Q. Wei, and X. J. Liu, "Ultra-sparse metasurface for high reflection of low-frequency sound based on artificial Mie resonances," Nat. Mater. 14(10), 1013–1019 (2015).
[5]J. He, Z. Zhou, C. Zhang, Y. Zheng, Y. Li, Y. Li, X. Jiang, and D. Ta, "Ultrasparse and omnidirectional acoustic ventilated metabarrier," Appl. Phys. Lett. 120(19), 191701 (2022).
[6]M. Sun, X. Fang, D. Mao, X. Wang, and Y. Li, "Broadband acoustic ventilation barriers," Phys. Rev. Appl 13(4), 044028 (2020).
[7]R. Dong, D. Mao, X. Wang, and Y. Li, "Ultrabroadband acoustic ventilation barriers via hybrid-functional metasurfaces," Phys. Rev. Appl. 15(2), 024044 (2021).
[8]C. Liu, J. Shi, W. Zhao, X. Zhou, C. Ma, R. Peng, M. Wang, Z. H. Hang, X. Liu, J. Christensen, N. X. Fang, and Y. Lai, "Three-dimensional soundproof acoustic metacage," Phys. Rev. Lett. 127(8), 084301 (2021).
[9]H. Long, Y. Zhu, Y. Gu, Y. Cheng, and X. Liu, "Inverse design of an ultrasparse dissipated-sound metacage by using a genetic algorithm," Phys. Rev. Appl. 18(4), 044032 (2022).
[10]C. Shen, Y. Xie, J. Li, S. A. Cummer, and Y. Jing, "Acoustic metacages for sound shielding with steady air flow," J. Appl. Phys. 123(12), 124501 (2018).
[11]R. J. Astley and A. Cummings, "A finite element scheme for attenuation in ducts lined with porous material: Comparison with experiment," J. Sound Vib. 116(2), 239–263 (1987).
[12]X. Yu, L. Cheng, and X. You, "Hybrid silencers with micro-perforated panels and internal partitions," J. Acoust. Soc. Am 137(2), 951–962 (2015).
[13]X. Yu, S. K. Lau, L. Cheng, and F. Cui, "A numerical investigation on the sound insulation of ventilation windows," Appl. Acoust. 117, 113–121 (2017).
[14]I. Lee, A. Selamet, and N. T. Huff, "Impact of perforation impedance on the transmission loss of reactive and dissipative silencers," J. Acoust. Soc. Am. 120(6), 3706–3713 (2006).
[15]M. Yang and P. Sheng, "Sound absorption structures: From porous media to acoustic metamaterials," Annu. Rev. Mater. Res. 47(1), 83–114 (2017).
[16]S. A. Cummer, J. Christensen, and A. Alu, "Controlling sound with acoustic metamaterials," Nat. Rev. Mater. 1(3), 16001 (2016).
[17]B. Assouar, B. Liang, Y. Wu, Y. Li, J. C. Cheng, and Y. Jing, "Acoustic metasurfaces," Nat. Rev. Mater. 3(12), 460–472 (2018).
[18]L. Li, B. Zheng, L. Zhong, J. Yang, B. Liang, and J. Cheng, "Broadband compact acoustic absorber with high-efficiency ventilation performance," Appl. Phys. Lett. 113(10), 103501 (2018).
[19]M. Yang, C. Meng, C. Fu, Y. Li, Z. Yang, and P. Sheng, "Subwavelength total acoustic absorption with degenerate resonators," Appl. Phys. Lett. 107(10), 104104 (2015).
[20]C. Fu, X. Zhang, M. Yang, S. Xiao, and Z. Yang, "Hybrid membrane resonators for multiple frequency asymmetric absorption and reflection in large waveguide," Appl. Phys. Lett. 110, 021901 (2017).
[21]X. Xiang, X. Wu, X. Li, P. Wu, H. He, Q. Mu, S. Wang, Y. Huang, and W. Wen, "Ultra-open ventilated metamaterial absorbers for sound-silencing applications in environment with free air flows," Extrem. Mech. Lett. 39, 100786 (2020).

[22]X. Xiang, H. Tian, Y. Huang, X. Wu, and W. Wen, "Manually tunable ventilated metamaterial absorbers," Appl. Phys. Lett. 118(5), 053504 (2021).
[23]A. D. Lapin, "Monopole-dipole type resonator in a narrow pipe," Acoust. Phys. 49(6), 731–732 (2003).
[24]H. Long, Y. Cheng, and X. Liu, "Asymmetric absorber with multiband and broadband for low-frequency sound," Appl. Phys. Lett. 111, 143502 (2017).
[25]T. Lee, T. Nomura, E. M. Dede, and H. Iizuka, "Asymmetric loss-induced perfect sound absorption in duct silencers," Appl. Phys. Lett. 116(21), 214101 (2020).
[26]T. Lee, T. Nomura, E. M. Dede, and H. Iizuka, "Ultrasparse acoustic absorbers enabling fluid flow and visible-light controls," Phys. Rev. Appl. 11(2), 024022 (2019).
[27]X. Su and D. Banerjee, "Extraordinary sound isolation using an ultrasparse array of degenerate anisotropic scatterers," Phys. Rev. Appl. 13(6), 064047 (2020).
[28]A. D. Lapin, "Sound absorption by monopole-dipole resonators in a multimode waveguide," Acoust. Phys. 51(3), 362–364 (2005).
[29]J. R. Piper, V. Liu, and S. Fan, "Total absorption by degenerate critical coupling," Appl. Phys. Lett. 104, 251110 (2014).
[30]M. Yang, Y. Li, C. Meng, C. Fu, J. Mei, Z. Yang, and P. Sheng, "Sound absorption by subwavelength membrane structures: A geometric perspective," C. R. Mec. 343(12), 635–644 (2015).
[31]S. Huang, S. Xie, H. Gao, T. Hao, S. Zhang, T. Liu, Y. Li, and J. Zhu, "Acoustic Purcell effect induced by quasibound state in the continuum," Fundamental Res. (published online 2022).